EGU General Assembly 2024 – Vienna, Austria & Online
G4.2 Modern Concepts for Ground and Space Observations of the Earth Gravity Field
EGU24-19344 (X2.32)
DOI:10.5194/egusphere-egu24-19344

Sharing is encouraged

Detecting the co-seismic and post-seismic gravity signal of large thrust earthquakes with Quantum Space Gravimetry mission concepts

Alberto Pastorutti[1], Carla Braitenberg[1]
[1] Univ. Trieste, Dept. of Mathematics, Informatics and Geosciences, Trieste, Italy

1 Introduction & aim

In the context of modelling and analyzing the gravity effect of earthquakes, we present the output of a forward modelling segment and an example of its use in the simulations of a Quantum Space Gravimetry mission. The aim of the former, the modelling segment, is:

- providing **updates to the solid Earth component of the AOHIS** model (Dobslaw et al., 2015), to be used in mission simulations
- assessing the **retrievability of the forward modelled earthquake signals** in a closed-loop setup
- formulating the required **signal levels for Mission Requirements Documents**
- assessing the added **value of satellite gravimetry in the inversion of co- and post-seismic movements**, complementing seismological estimates and data from other geodetic observables

We modelled the co-seismic mass change and effect on gravity of a first set of **"benchmark earthquakes", real events that we use to construct a set of realistic synthetics signals**. We devised a procedure, relying on the **QSSPSTATIC** code (Wang et al., 2017), which allows reading source data as from point-source or finite fault solutions and producing **global grids and spherical harmonics (SH) coefficients of the change in geopotential and its derived quantities.**

The **post-seismic signal due to mass change resulting from visco-elastic relaxation is also modelled**. While the signal levels are at least one order of magnitude smaller than co-seismic signals (depending on the observed time window), they are of particular interest due to their a-seismic behaviour and the difficulty of being sensed when direct estimates of surface deformation are not available - e.g. offshore.

We also show an experiment on the effect of omitting the complexity of a fault with finite dimensions, significant variations of slip throughout the fault plane and multiple fault planes. **We test how an approximated source model affects the estimated signal.**

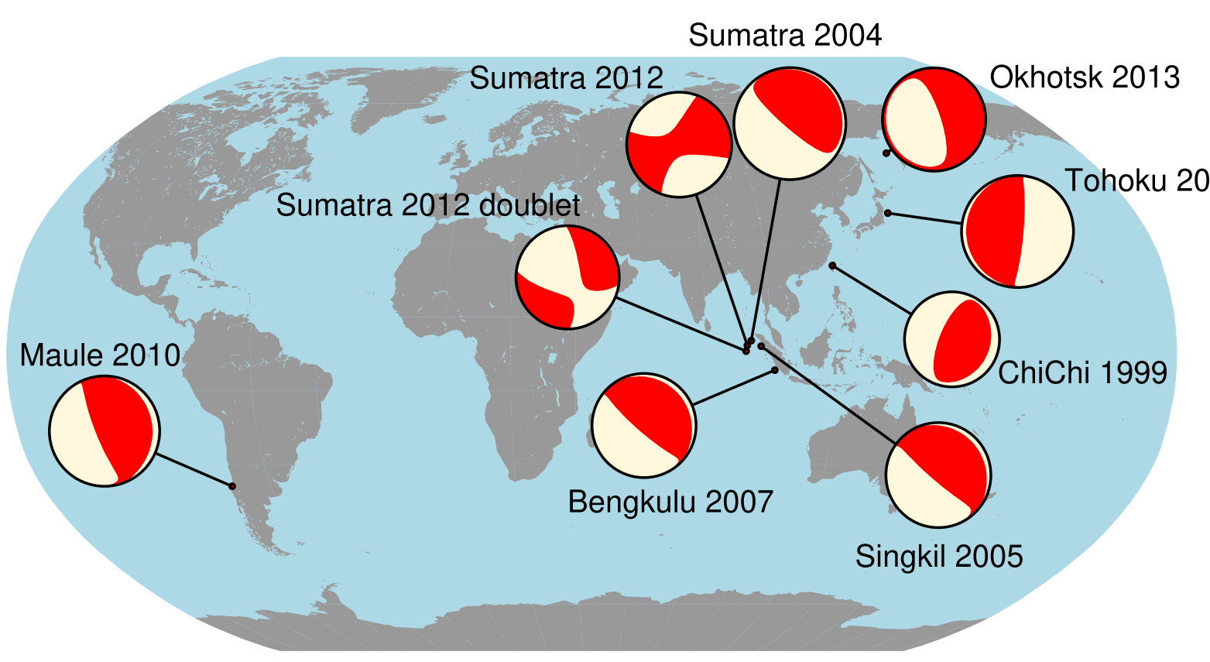

We used the output of the forward modelling in a **detectability assessment segment, in which we compare the earthquake signals with the output of simulations in the Quantum Space Gravimetry for monitoring Earth's Mass Transport Processes (QSG4EMT).**

Owing to the coloured error spectra of gravity models and thus aiming at detecting our signals in the optimal range of spatial scales, where the error of the gravity models is smaller, we employ a spectral, spherical harmonic domain, analysis method, adapted for signals with strong regional footprints that require **spatio-spectral localization** before performing spectral comparisons (e.g. Han & Ditmar, 2008).

Since the signals modelled here were included in simulations, we can also **assess if the earthquakes can be retrieved from the simulated weekly gravity products**, for different constellations.

2 Modeling strategy

Earthquake modelling code
We adopt the QSSPSTATIC code by Wang et al. (2017), which allows modelling of long-term deformation, including viscoelastic post-seismic relaxation. Provided with a rheological model, source parameters, and location of receivers (computation points), it computes the time series of a number of geodetic observables in each receiver point, according to the requested time sampling and total time span. Change in radial gravity is among them, expressed as the attraction of the displaced masses ("inertial effect") with no other effects (e.g. movement of a ground-tied gravimeter).

Input data
We read the earthquake source definition either as a point source, optionally by parsing a list of quakeML files, or the description of a finite fault solution (in CMT and Coulomb format). These are transformed in the QSSP INP-file format, as source entries.

Global grids and SH analysis
To compute the SH expansion with a consistent coverage over all degrees, even the lower range, we distribute our computations points globally. The grid step is densified in a 20° × 20° area around the earthquake source, with an equiangular grid step of 0.0625°, to which the entire global grid is then interpolated. The global grids, expressed in terms of change in gravity disturbance, are transformed to their SH coefficients, which are then transformed to unitless SH coefficients of the change in potential.
Since the computation of observables at each source-receiver couple is independent, we employ a process-based parallelism setup, spreading a large number of computation points on different workers - resulting in a considerable speed up.

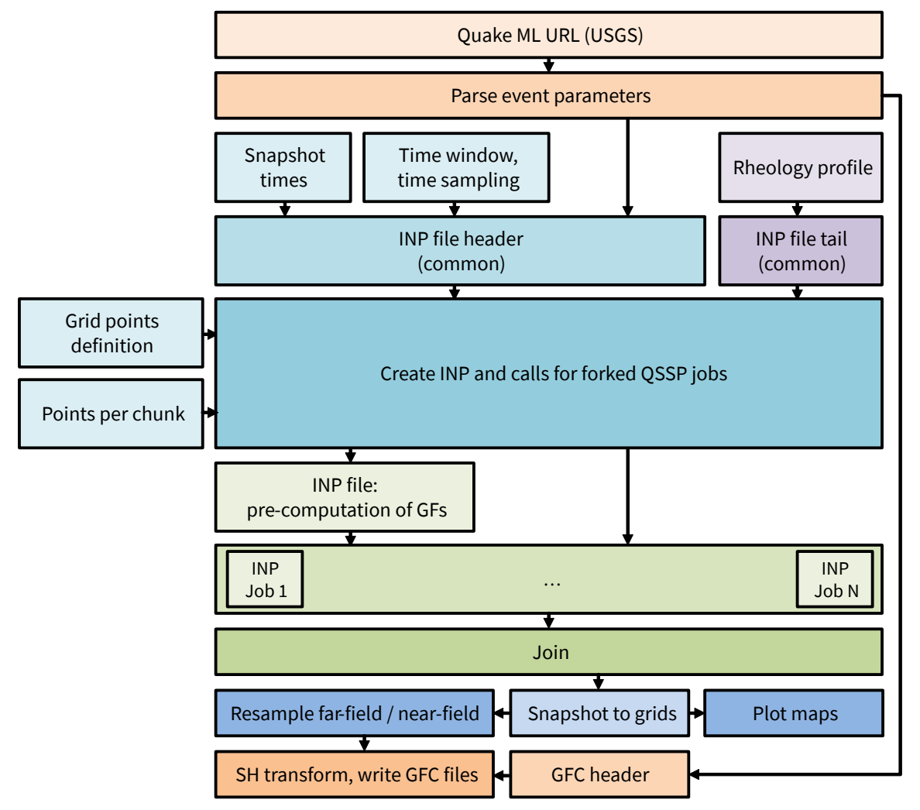

Above: computational flowchart for a point source.

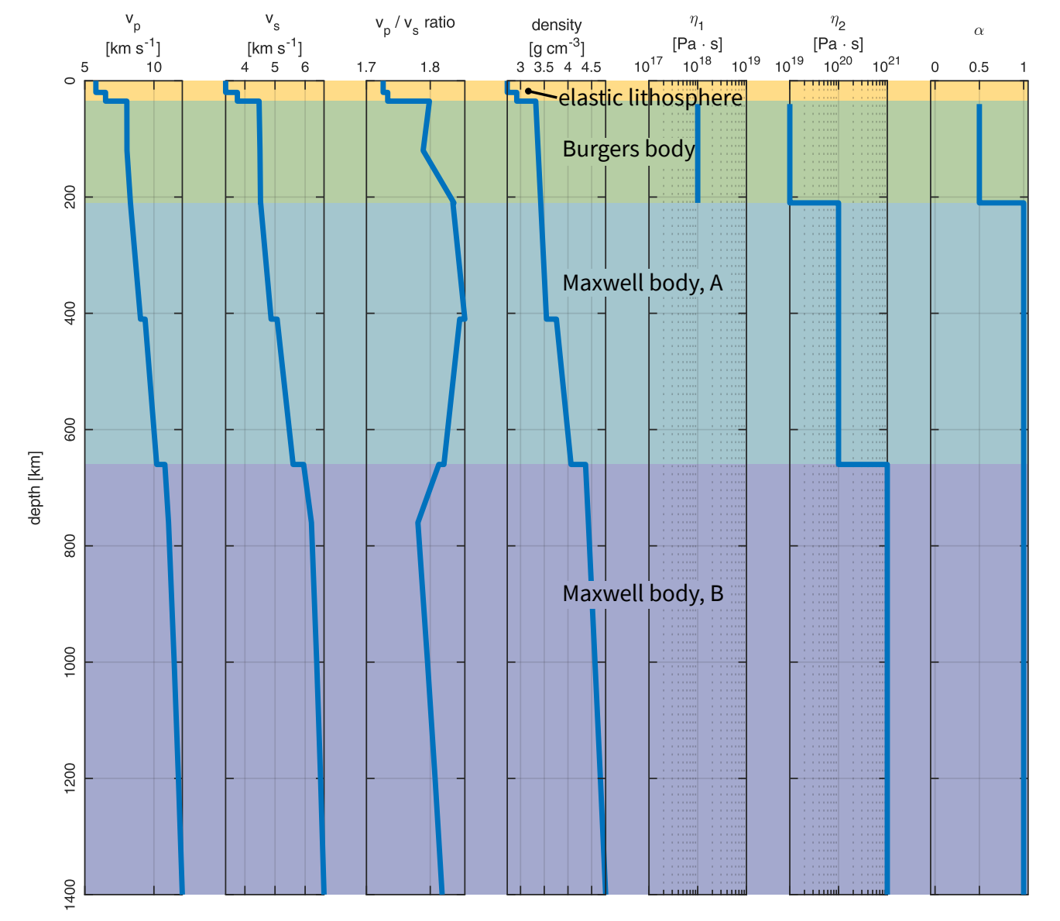

1-D rheological column
The model allows for a laterally uniform layered sphere.
In the tests presented here, beneath a purely elastic, 50 km thick lithosphere, we include a Burgers body rheology upper mantle (a Kelvin-Voigt body and a Maxwell body in series), modelling a relaxation of the shear modulus in time. Two Maxwell bodies, with increasing viscosity, are placed in the rest of the mantle.

Output formats
To allow the signals to be used in updating the Earth System Model used in simulations, the resulting fields are provided as global grids, unfiltered, in NetCDF format, and as truncated SH expansions, in GFC format. Both have the relevant metadata populated in their header. A snapshot of the global field is computed for a given range of times following the co-seismic change.

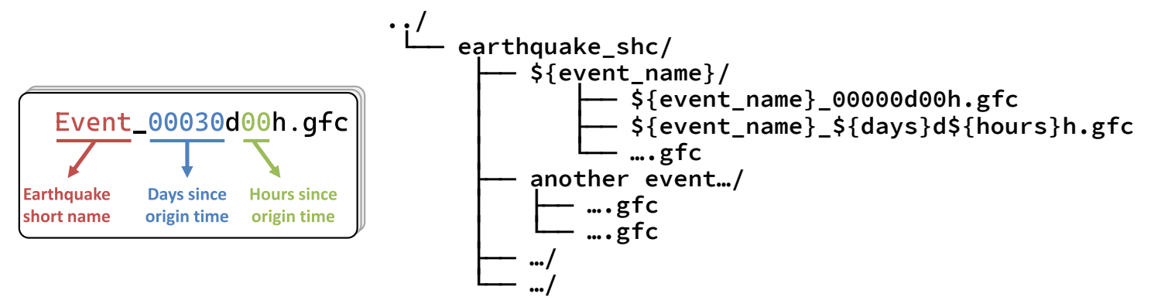

```
../
└── earthquake_shc/
    ├── ${event_name}/
    │       ├── ${event_name}_00000d00h.gfc
    │       ├── ${event_name}_${days}d${hours}h.gfc
    │       └── ….gfc
    ├── another event…/
    │   ├── ….gfc
    │   └── ….gfc
    ├── …/
    └── …/
```

3 Spectral domain "open-loop" detectability assessment

Target signal against average simulation retrieval errors

On the SH coefficients of each earthquake, at the time intervals under test (time since event and time span of a gravity product), we apply a windowing function according to the **spatio-spectral localization** by Wieczorek & Simons (2005), using a 9° radius spherical cap.

We compare our signals with four simulated scenarios (1, 2, 3, 6 satellite paris). SH degree error spectra are obtained from the **HIS retrieval error** of each simulation, expressed as the misfit between the retrieved and the mean true HIS signal in the same period of time.

All spectra in this section are expressed in non-cumulative per-degree RMS of the change in gravity, expressed as the first radial derivative of the disturbing potential (T_r).

7-day solutions and 7 days of co+post seismic signal

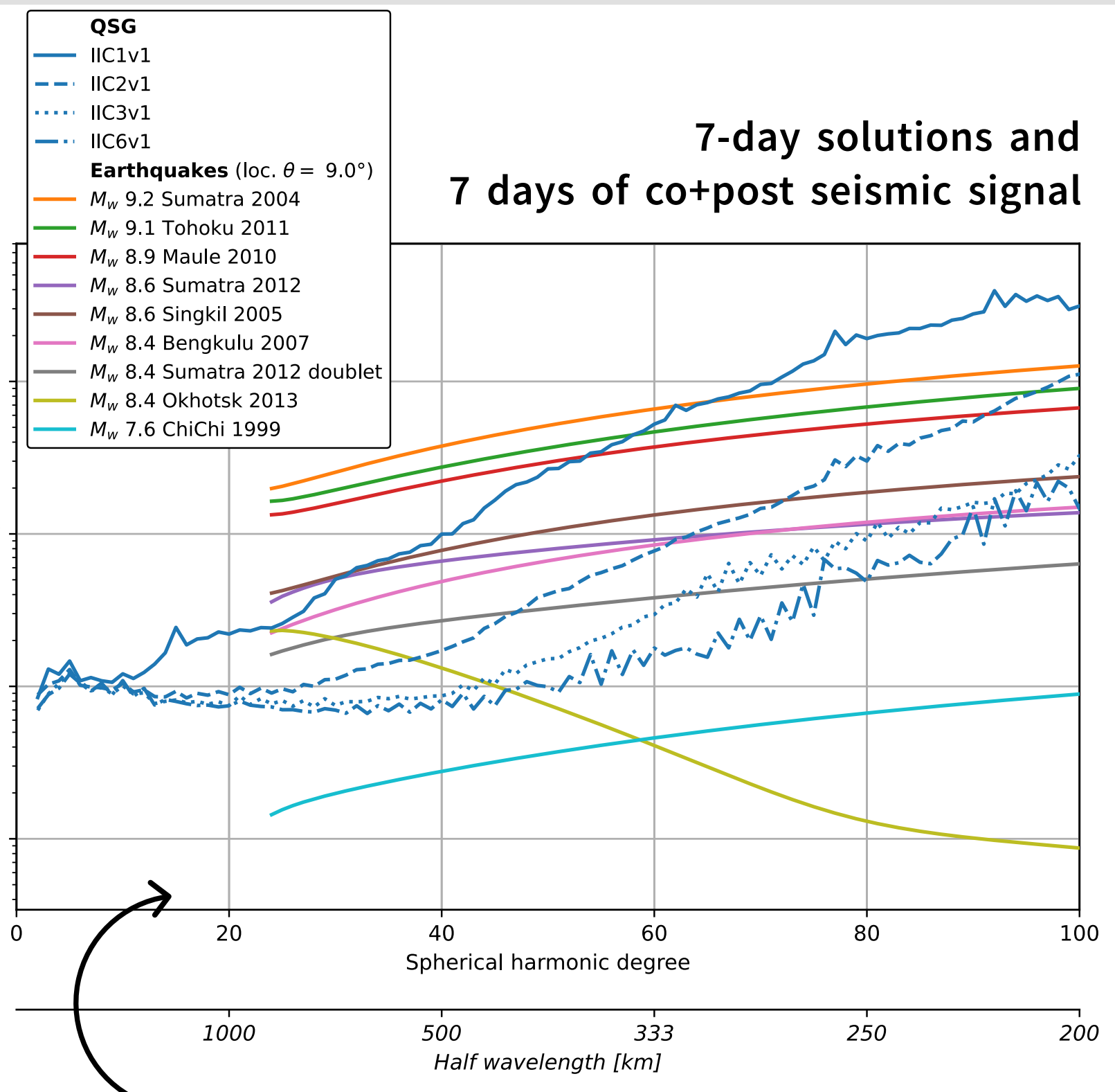

Short-term detectability of co-seismic change

A single pair would detect all the largest events ($M_w \geq 8.6$). A denser constellation of inclined pairs lowers the short-term detactability threshold. In addition to that, the spatial resolution is greatly improved.

30-day solutions and 30 days of post-seismic signal

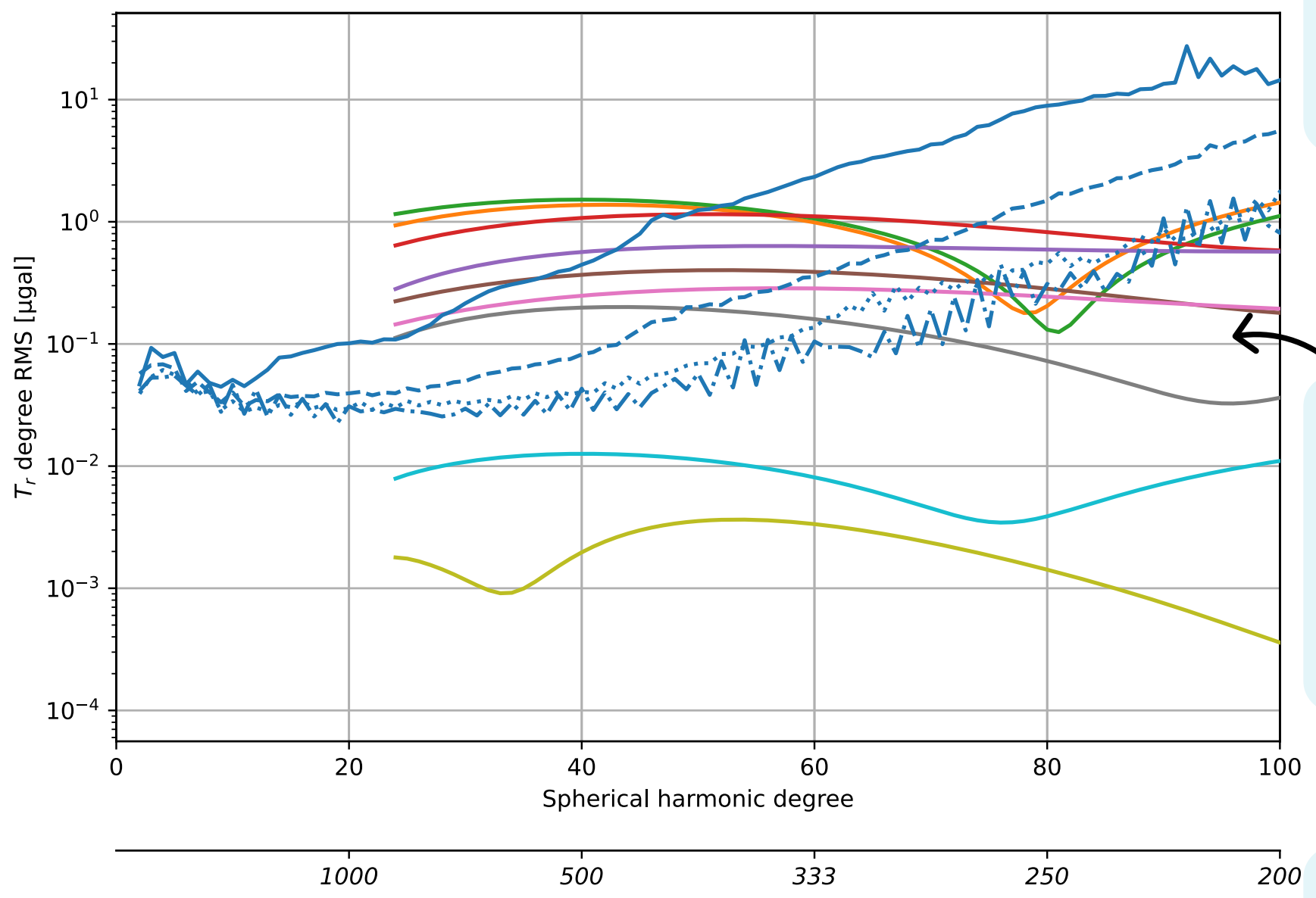

Short-term detectability of post-seismic change

In a 30-day time span, both in the gravity products and in the post-seismic signal (co-seismic removed), the detectability improves for almost all the events, also in terms of maximum detectable degree. The post-seismic signal is usually smaller than the co-seismic (the ratio depending on various factors, including depth), but this is compensated by the decrease in retrieval errors (by a factor close to the square root of the ratio between the compared timespans).

Post-seismic detectability through time

SNR = 1 contours, ticks towards SNR > 1

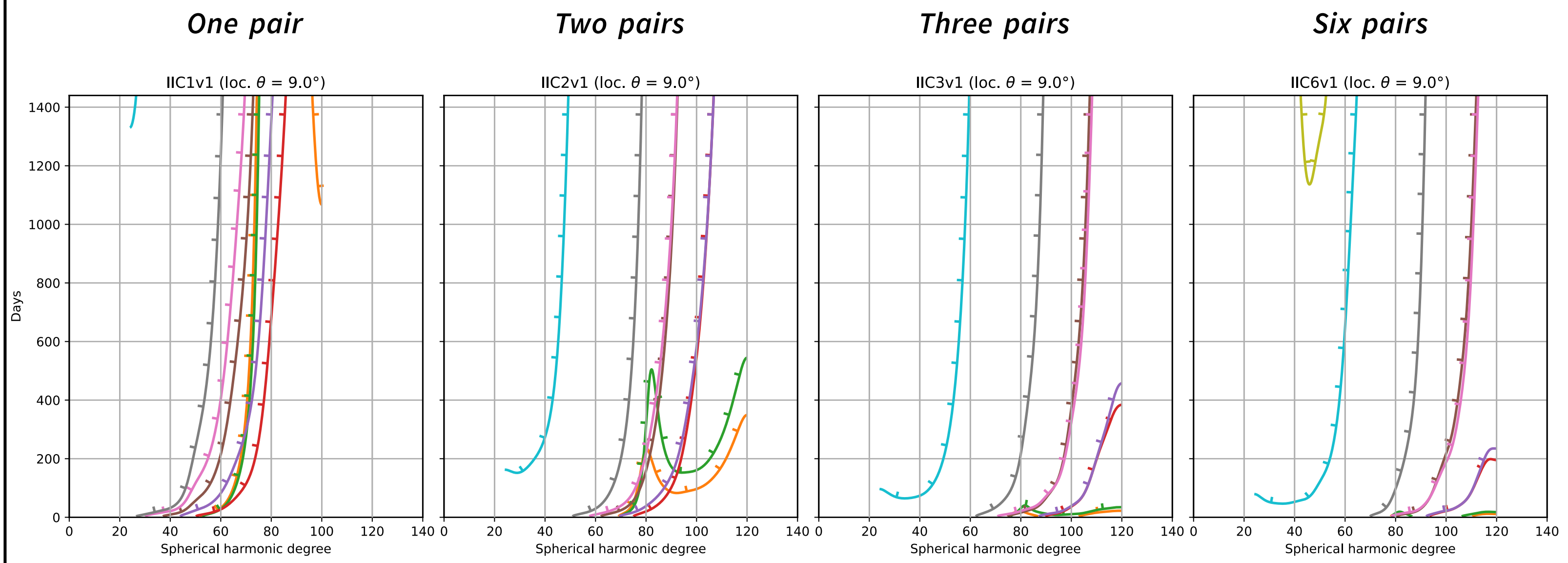

Long-term detectability of post-seismic change

Detectability of the isolated post-seismic visco-elastic relaxation, respect to the covered time span, in days since the event. **Each horizontal "slice" of constant days is equivalent to a spectrum plot**, as those shown above, from which the signal-error intersections are extracted. Note that **the post-seismic signal of the deep-focus earthquake in Okhotsk (2013) becomes detectable only with a 6-pair configuration** and years of observations, while **the shallow events with the same magnitude are detectable from the beginning.**

References

Daras I., March G., Pail R., Hughes C. W., Braitenberg C., Güntner A., Eicker A., Wouters B., Heller-Kaikov B., Pivetta T., Pastorutti A., 2014. Mass-change And Geosciences International Constellation (MAGIC) expected impact on science and applications, Geophysical Journal International, 236(3), https://doi.org/10.1093/gji/ggad472

Wang, R., Heimann, S., Zhang, Y., Wang, H., & Dahm, T., 2017. Complete synthetic seismograms based on a spherical self-gravitating Earth model with an atmosphere-ocean-mantle-core structure, Geophysical Journal International , 210(3), 1739{1764 https://doi.org/10.1093/gji/ggx259.

Dobslaw, H., Bergmann-Wolf, I., Dill, R., Forootan, E., Klemann, V., Kusche, J. & Sasgen, I., 2015. The updated ESA Earth System Model for future gravity mission simulation studies, J. Geod., 89(5), 505–513. https://doi.org/10.1007/s00190-014-0787-8.

Han, S. C. & Ditmar, P., 2008. Localized spectral analysis of global satellite gravity fields for recovering time-variable mass redistributions, Journal of Geodesy, 82(7), https://doi.org/10.1007/s00190-007-0194-5.

Eshelby, J., 1957. The determination of the elastic field of an ellipsoidal inclusion, and related problems, Proceedings of the Royal Society of London. Series A. Mathematical and Physical Sciences, 241(1226) https://doi.org/10.1098/rspa.1957.0133

Cambiotti, G., Douch, K., Cesare, S., Haagmans, R., Sneeuw, N., Anselmi, A., … Sabadini, R. (2020). On Earthquake Detectability by the Next-Generation Gravity Mission. Surveys in Geophysics, 41(5), 1049–1074. https://doi.org/10.1007/s10712-020-09603-7

Wieczorek, M. A. & Simons, F. J., 2005. Localized spectral analysis on the sphere, Geophysical Journal International , 162(3), https://doi.org/10.1111/j.1365-246X.2005.02687.x

4 Retrieval test: signal in the simulated products

Direct difference between solutions

We compute the observed (simulated) change as a difference between solutions: after (S_{n+1}) minus before (S_{n-1}). We then compare the reference co-seismic gravity change (plus short-term post-seismic) with respect to the simulated signal. We synthesise these signals, from their SH expansions, using a **tapered truncation between SH degrees 40 and 80**, i.e. we low-pass in the range where the one-pair case already shows positive detectability of this event.

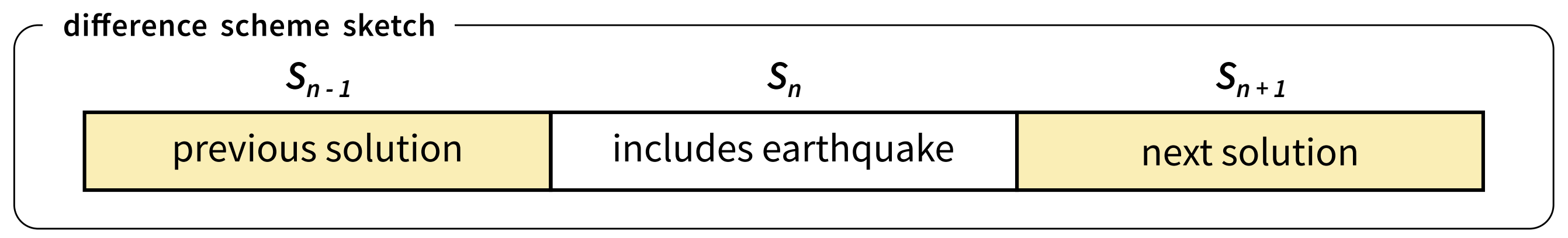

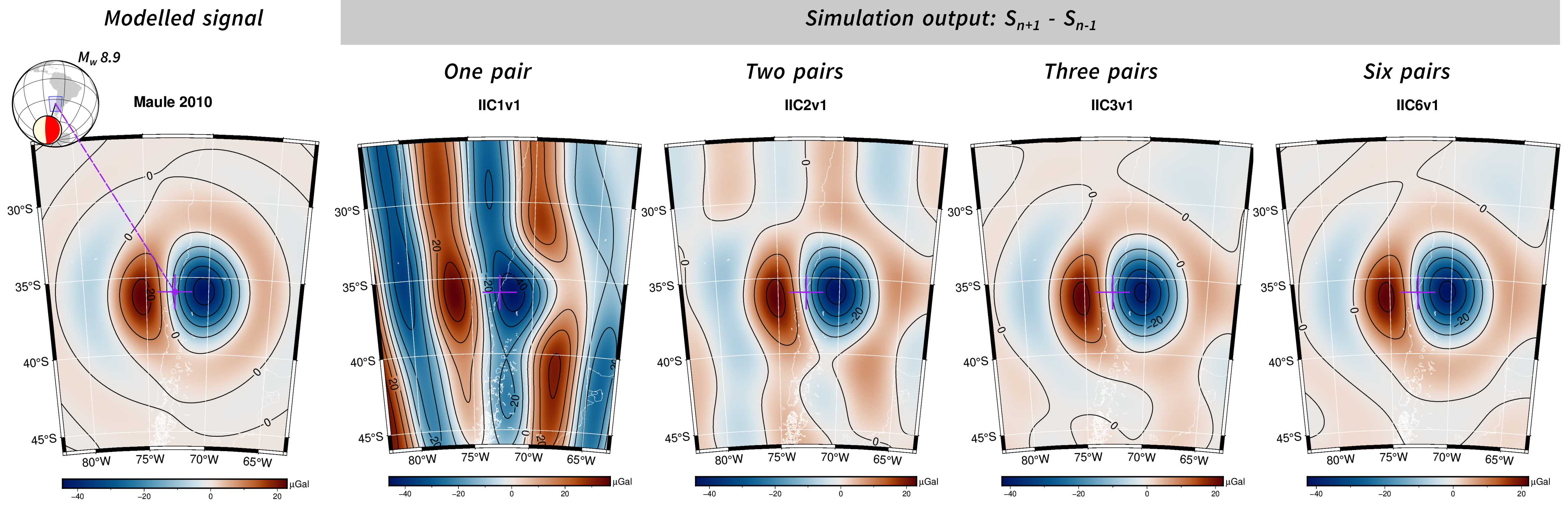

If we further subtract to this "direct difference" the difference between the simulation input signals (earthquakes and HIS), we can isolate the retrieval residuals. We compute the min, max, and RMS metrics in 10° × 10° rectangle around the source.

One pair	Two pairs	Three pairs	Six pairs
-31.88/29.23/18.32	*-4.52/5.36/1.35*	*-1.39/1.33/0.57*	*-0.71/1.56/0.49*

Time-domain fitting

As a complimentary strategy, simulating a **signal separation** approach, we **fit a time dependent function** to the serie of observed gravity - this can be done both in the spectral- and in the spatial-domain (on Stokes' coefficients and on elements of the synthesized grids, respectively). Here we show an example in which we perform a spatial-domain fit, presenting the output on a selected point: the east (negative) peak of Maule (2010) co-seismic.

The model function is the following:

$$k+mt_d+a_1\sin(2\frac{\pi}{y_d}t_d)+b_1\cos(2\frac{\pi}{y_d}t_d)+a_2\sin(2\frac{\pi}{y_d/2)}t_d)+ b_2\cos(2\frac{\pi}{y_d/2)}t_d)+h\Theta(t_d-h_{shift})$$

t_d time in days
y_d year (in days)
Θ Heaviside step function

This can serve as a starting point to fit the post-seismic relaxation (by isolating it from the other superimposed signals) or to assess the performance of fitting time-varying signals in the different mission scenarios, where larger retrieval errors hinder a reliable fit.

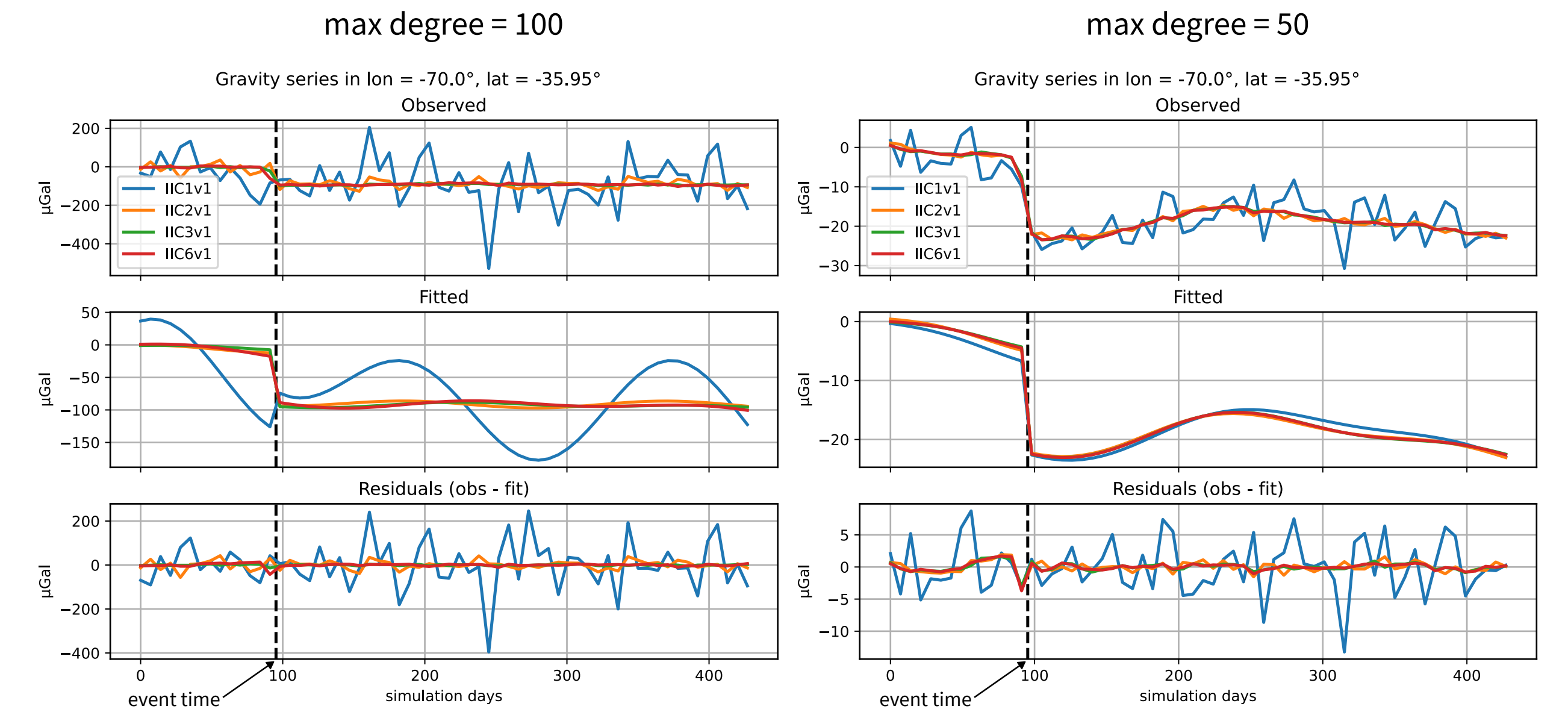

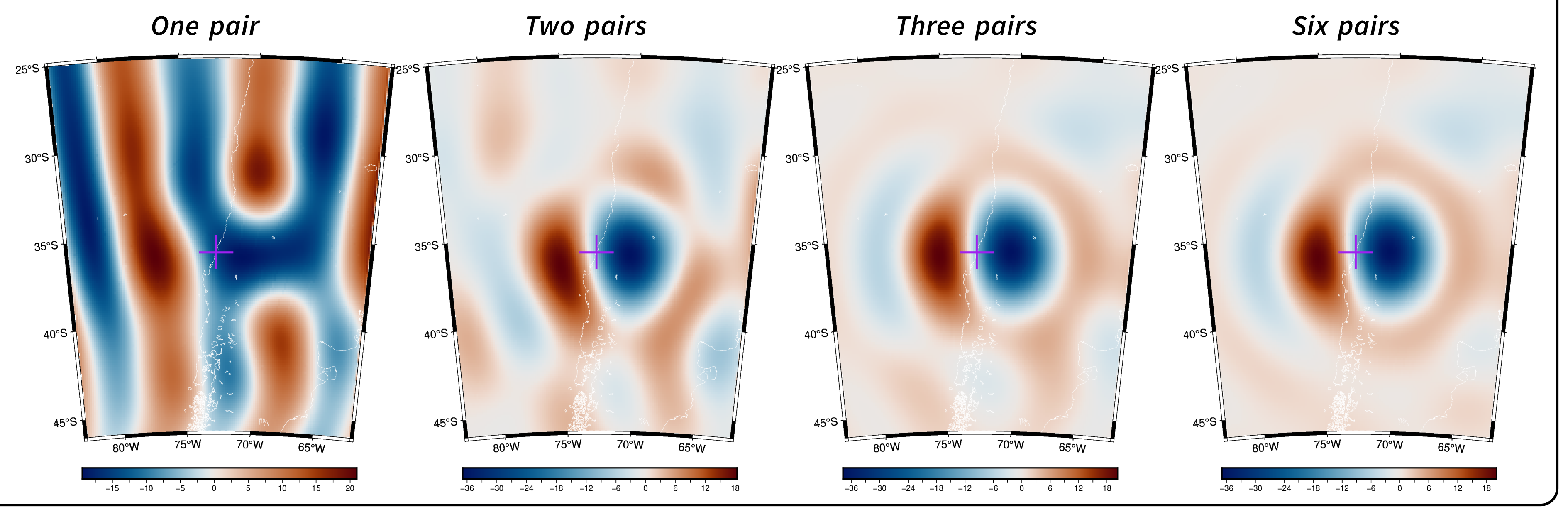

Fitted value of h, co-seismic change

Here the fitted value (in µGal) for the parameter h is plotted for all the points in the area, each point constituting a separately fitted time serie. The retrieved earthquake signal through time-domain fitting is coherent with the result of direct difference between timestep, with the collateral of allowing to estimate other time-varying components.

UNIVERSITÀ DEGLI STUDI DI TRIESTE

This work is part of the Solid Earth applications assessment of ESA-funded project **Quantum Space Gravimetry for monitoring Earth's Mass Transport Processes (QSG4EMT)**
`asg.ed.tum.de/iapg/qsg4emt`

Computational resources for part of the work presented herein were provided by the infrastructure of MIGe, UniTS (Argo cluster) and the Ulysses HPC cluster of SISSA, under a SISSA-MIGe agreement.

contact: apastorutti@units.it, berg@units.it
Tectonophysics & Geodynamics Research Group
Dept. of Mathematics, Informatics and Geosciences, Univ. of Trieste
via Edoardo Weiss, 1 - 34128 Trieste (Italy)